

Estimation of Lane Data-based Features by Odometric Vehicle Data for Driver State Monitoring

Fabian Friedrichs and Michael Miksch and Bin Yang

Chair of System Theory and Signal Processing
University of Stuttgart, Germany

Abstract—It is assumed that approximately one third of severe car accidents are related to drowsiness. Warning systems such as the Mercedes Benz Attention Assist try to tackle this problem by analyzing the driving style. Previous work investigated the estimation of measures (features) from lane data that correlate well with impaired driving. Unfortunately, these features require a lane-tracking camera, which is not available in many cars. Furthermore, the lane data signals are often affected from missing road markings, bad sight etc. Some lane-based features such as LANEDEV or ZIGZAGS do not require the absolute distance to the lane markings, but only depend on the lateral deviation within the lane. Our idea is to exploit odometric data (yaw rate and vehicle speed) to estimate this measure. The vehicle trajectory is a composition of the lurching between lane markings and the disturbing road curvature. Thus, we remove this curvature by a filter since its frequency is lower than the vehicle deviation. We compare the correlation between features based on lane data and odometric data as well as their relationship with sleepiness. An excerpt of the Attention Assist database with 294 drives and over 76 000 km is used. We show that some lane-based features can be approximated well. The zero-crossing rate (LATPOSZCR) performs even better than its lane-based pendant.

Keywords: drowsiness detection, driver monitoring, odometric data, tracking, extended kalman filter, classification.

I. INTRODUCTION

A. Motivation

The vast majority of road accidents are primarily related to mistakes by the driver. The 100-Car Study, performed in 2006 by the National Highway Traffic Safety Administration NHTSA [1] and Virginia Tech Transportation Institute (VTTI), state that drowsiness increases the driver's risk of a crash or near-crash by at least a factor of four. According to the NHTSA about 100,000 crashes are annually the result of driver sleepiness. Experts assume that about 24-33% of the severe accidents are related to drowsiness [2]–[5]. Emerging driver monitoring systems, such as the Mercedes Benz *Attention Assist*, are systems that aim to reduce sleepiness related road crashes caused by fatigued and distracted drivers by using standard equipment sensors. In order to develop and optimize such systems, a reliable and accurate sleepiness reference is needed. There are several common ways to record the driver's vigilance state. The most common

reference measure for drowsiness is the driver's subjective self-evaluation according to the Karolinska Sleepiness Scale (KSS) [6] in Tab. I.

TABLE I
KAROLINSKA SLEEPINESS SCALE (KSS)

KSS	Description
1	Extremely alert
2	Very alert
3	Alert
4	Rather alert
5	Neither alert nor sleepy
6	Some signs of sleepiness
7	Sleepy, no effort to stay awake
8	Sleepy, some effort to stay awake
9	Very sleepy, great effort to keep awake, fighting sleep

Previous work [7], [8] investigated the estimation of features from lane data that correlate well with impaired driving. The problem about these features is that they require a lane-tracking camera, which is only available as special equipment in few vehicles. Furthermore, the lane data signals are often affected due to missing road markings, bad weather and light conditions or a miss-calibrated camera. Some lane-based features such as LANEDEV, ZIGZAGS and others do not require the absolute position towards the lane markings. It is sufficient to know the deviation within the lane. Thus, this article investigates the use of odometric vehicle data only to calculate the classical lane-based features without the need of a lane-tracking camera. We also refer to the sensor signals of odometric data as *inertial* data. The basic assumption behind this approach is that the curvature of the road can be estimated from the odometric data. As described in [9], there is a minimum curvature radius for every speed limit. For instance the minimum curvature radius at 120km/h is 750 meters. In general, this is considered during road construction, so we can assume that the road curvature has low frequencies in the vehicle trajectory. The lane deviation was observed to occur at much higher frequencies, so it can be extracted by a high-pass filter. To estimate the vehicle trajectory, we use an extended Kalman filter and a vehicle motion model.

In addition to yaw rate and vehicle speed, the vehicle's GPS position is also included. GPS was converted to UTM to have the same metric coordinate system as the coupled odometric position. This is valuable for visualization and in order to evaluate the system performance, but will not be needed in the online system.

F. Friedrichs, M. Miksch and Prof. B. Yang are with Faculty of Electrical Engineering, Chair of System Theory and Signal Processing, University of Stuttgart, Pfaffenwaldring 47, 70550 Stuttgart, Germany, {fabian.friedrichs, michael.miksch, bin.yang}@lss.uni-stuttgart.de. This work was supported by Daimler AG, Mercedes-Benz Car Group

Many other aspects in regards to drowsiness detection profit by this improved vehicle position. Short lane-tracking gaps can be filled and road-condition analyses benefits from this improved spatial resolution.

In this study, an excerpt of the Mercedes Benz Attention Assist database with 294 drives and over 76 thousand kilometers was used.

B. Literature review

Within the last years, a lot of effort has been made to investigate driver monitoring based on steering behavior, lane-keeping and blinking behavior. For a review on driver monitoring literature see [7], [8]. There are many approaches for vehicle tracking with inertial vehicle data. Hasberg [10] uses splines and a Kalman filter for online estimation of train tracks. Bühren [11] investigated the tracking of vehicle target lists by radar. Miksch et. al. [12] used a vehicle motion model to estimate the ego-motion for motion compensation. However, no literature was found that analyzed the estimation of lane-based features from inertial vehicle data.

C. Objectives of the current study

This study is focusing on the following objectives:

- Estimate the relative lateral lane position (deviation within the lane) by using odometric CAN-data such as the yaw rate and wheel rotation speed.
- Provide mathematical background on how to estimate the vehicle trajectory.
- Compare the performance of odometric features and their classical lane-based pendant.
- The goal is *not* to find new features based on odometric data, but to compare and replace proven lane-based features without the need of a lane-tracking camera.

D. Database

The database used within this project covers over 17 800 real-road drives with a driven distance of over 1.67 Mio km (courtesy of Mercedes-Benz). After filtering this database for drives over 30km, with valid and plausible drowsiness self-rating (KSS), valid lane-tracking data and without measurement errors, 76 215km of real drives remained.

- 294 drives (37 night experiment drives)
- 11 vehicles (Seven E- and five S-Class)
- 94 drivers

Fig. 1 shows a map of the drives in Europe.

The conduction of night experiments and regular drives is explained in [7], [13].

II. IMPLEMENTATION DETAILS

In order to obtain the lateral lane position signal from odometric data, the processing steps presented in this section are proposed.

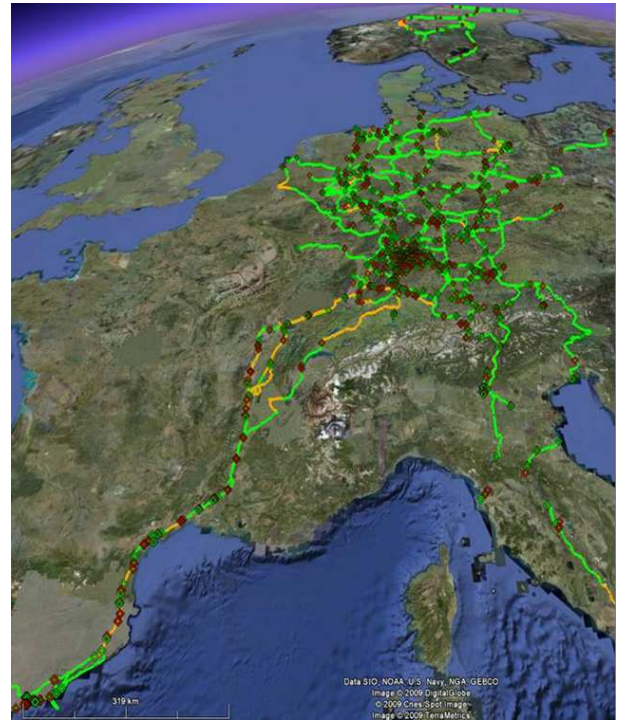


Fig. 1. Map of drives: green lines indicate *awake* driving sections, orange indicate *questionable* and red *drowsy* sections

A. Sensor Signals and Synchronization

The yaw rate sensor has a sampling frequency of $F_s = 1/T \approx 50\text{Hz}$. The GPS signals were available with a sampling rate of $F_s = 1/T \approx 1\text{Hz}$ and not always valid. Every second, when new GPS data were available, an additional modified Kalman iteration is called to update the position according to the GPS data. This way, the Kalman filter takes over the weighting between inertial data and GPS data.

B. State Space Model

Fig. 2 illustrates the motion model used in this article. As described in [11], [12], the vehicle motion can be modeled as follows. We choose the system model with the state transition equation

$$\mathbf{x}(k+1) = \mathbf{A}\mathbf{x}(k) \quad (1)$$

with the *state vector* $\mathbf{x}(k)$ at instant k . Refer to App. A for a summary of the used symbols. The second part of the system model is the measurement equation

$$\mathbf{z}(k+1) = \mathbf{H}\mathbf{x}(k) \quad (2)$$

with the *measurement vector* $\mathbf{z}(k)$ at instant k . The movement of the vehicle can then be described as

$$\begin{bmatrix} s_x(k+1) \\ s_y(k+1) \end{bmatrix} = \begin{bmatrix} s_x(k) \\ s_y(k) \end{bmatrix} + v^+(k)T \begin{bmatrix} \cos(\psi^+) \\ \sin(\psi^+) \end{bmatrix}. \quad (3)$$

Thereby we defined

$$v^+ = v(k) + a(k)\frac{T}{2} \quad \text{and} \quad \psi^+ = \psi + \dot{\psi}\frac{T}{2}$$

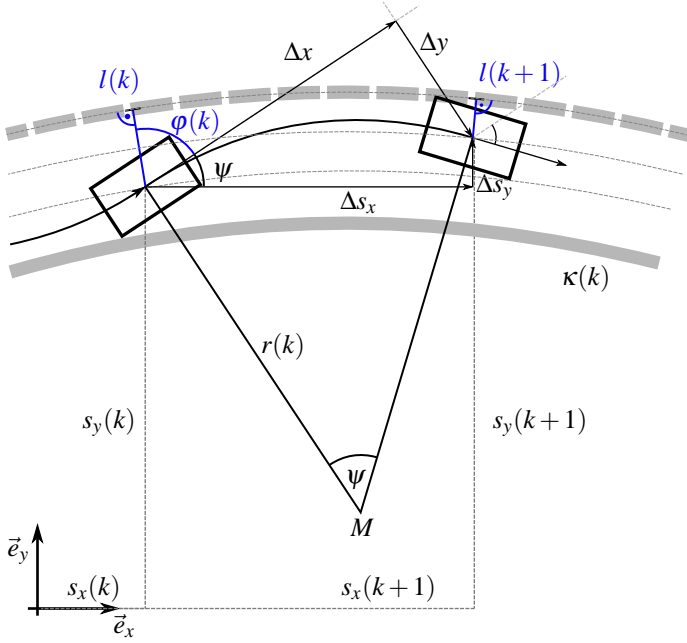


Fig. 2. Motion Model

with the cycle time T and the state vector

$$\mathbf{x}(k+1) = \begin{bmatrix} s_x(k+1) \\ s_y(k+1) \\ \psi(k+1) \\ \dot{\psi}(k+1) \\ \ddot{\psi}(k+1) \\ v(k+1) \\ a(k+1) \end{bmatrix} \begin{array}{l} \text{x-position} \\ \text{y-position} \\ \text{yaw angle} \\ \text{yaw rate} \\ \text{yaw jerk} \\ \text{longit. velocity} \\ \text{longit. acceleration} \end{array} \begin{array}{l} [m] \\ [m] \\ [^\circ] \\ [^\circ/s] \\ [^\circ/s^2] \\ [m/s] \\ [m/s^2] \end{array} \quad (4)$$

Finally, we can write the following equation that describes the state transition

$$\mathbf{f}(\mathbf{x}, \mathbf{q}) = \begin{bmatrix} s_x(k) + \cos(\psi^+) \cdot v(k)T \\ s_y(k) + \sin(\psi^+) \cdot v(k)T \\ \psi(k) + \dot{\psi}T \\ \dot{\psi}(k) + \ddot{\psi}(k)T \\ \ddot{\psi}(k) \\ v(k) + a(k)T \\ a(k) \end{bmatrix}.$$

The system is still non-linear so that the extended Kalman filter (EKF) is required. For the EKF, we need to linearize the non-linear, differentiable function \mathbf{f} in each working point, which is the current system state $\mathbf{x}(k)$. For linearization, the *Jacobi-Matrix* of the differentiable function $f: \mathbb{R}^n \rightarrow \mathbb{R}^m$ is needed and defined by

$$\mathbf{J}(\mathbf{f}) = \begin{bmatrix} \frac{\partial f_1}{\partial x_1} & \frac{\partial f_1}{\partial x_2} & \cdots & \frac{\partial f_1}{\partial x_n} \\ \vdots & \vdots & \ddots & \vdots \\ \frac{\partial f_m}{\partial x_1} & \frac{\partial f_m}{\partial x_2} & \cdots & \frac{\partial f_m}{\partial x_n} \end{bmatrix}. \quad (5)$$

Finally, we obtain for $\frac{\partial \mathbf{f}(\mathbf{x}, \mathbf{q})}{\partial \mathbf{x}}$:

$$\begin{bmatrix} 1 & 0 & -\sin(\psi^+)v^+T & -\sin(\psi^+)v^+ \frac{T^2}{2} & 0 & \cos(\psi^+)T & \cos(\psi^+) \frac{T^2}{2} \\ 0 & 1 & \cos(\psi^+)v^+T & \cos(\psi^+)v^+ \frac{T^2}{2} & 0 & \sin(\psi^+)T & \sin(\psi^+) \frac{T^2}{2} \\ 0 & 0 & 1 & T & 0 & 0 & 0 \\ 0 & 0 & 0 & 1 & T & 0 & 0 \\ 0 & 0 & 0 & 0 & 1 & 0 & 0 \\ 0 & 0 & 0 & 0 & 0 & 1 & T \\ 0 & 0 & 0 & 0 & 0 & 0 & 1 \end{bmatrix}.$$

Then, the measurement matrix \mathbf{H} and vector $\mathbf{z}(k)$ are

$$\mathbf{H} = [\mathbf{0} \quad \mathbf{I}], \quad \mathbf{z}(k) = \begin{bmatrix} \psi(k+1) \\ \dot{\psi}(k+1) \\ v(k+1) \\ a(k+1) \end{bmatrix}.$$

In case that a new GPS sample is available, the measurement matrix \mathbf{H} and vector $\mathbf{z}(k)$ were extended:

$$\mathbf{H} = \begin{bmatrix} 1 & 0 & & & & & \\ 0 & 1 & & & & & \\ & & \mathbf{0} & & & & \\ & & & \mathbf{I} & & & \end{bmatrix}, \quad \mathbf{z}(k) = \begin{bmatrix} U_e(k+1) \\ U_n(k+1) \\ \psi(k+1) \\ \dot{\psi}(k+1) \\ v(k+1) \\ a(k+1) \end{bmatrix}$$

where U_e and U_n are the *easting* and *northing* UTM coordinates. The covariance matrices \mathbf{Q} and \mathbf{R} have been chosen by using the high-passed measurements.

C. Optimal state estimation using the Kalman filter

The Kalman filter for linear systems is a tool to estimate the state vector that can be observed through indirect measurements which are disturbed by noise.

$$\mathbf{x}(k+1) = \mathbf{A}\mathbf{x}(k) + \mathbf{B}\mathbf{u}(k) + \mathbf{w}(k), \quad (6)$$

$$\mathbf{z}(k+1) = \mathbf{H}\mathbf{x}(k) + \mathbf{v}(k) \quad (7)$$

The model noise $\mathbf{w}(k)$ and measurement noise $\mathbf{v}(k)$ were found as additive normally distributed white noise

$$\begin{aligned} E[\mathbf{w}(n)\mathbf{w}^T(k)] &= \mathbf{W}\delta_{nk} \\ E[\mathbf{v}(n)\mathbf{v}^T(k)] &= \mathbf{V}\delta_{nk} \\ p(\mathbf{w}) &\propto \mathcal{N}(0, \mathbf{Q}) \\ p(\mathbf{v}) &\propto \mathcal{N}(0, \mathbf{R}) \end{aligned}$$

with zero mean

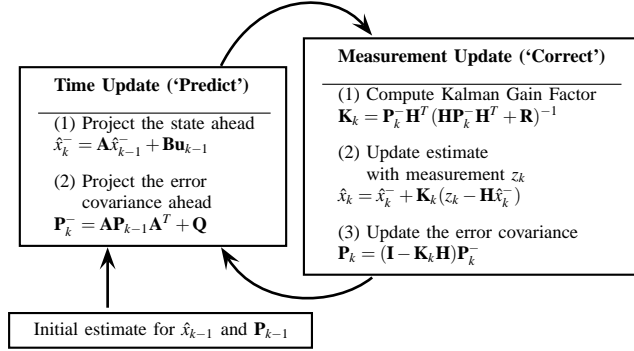
$$\begin{aligned} E[\mathbf{w}_n] &= \mathbf{0} \\ E[\mathbf{v}_n] &= \mathbf{0}. \end{aligned}$$

Model noise, measurement noise and initial states are uncorrelated:

$$\begin{aligned} E[\mathbf{w}(n)\mathbf{v}^T(n)] &= \mathbf{0} \\ E[\mathbf{w}(n)\mathbf{z}^T(n)] &= \mathbf{0} \\ E[\mathbf{v}(n)\mathbf{z}^T(n)] &= \mathbf{0}. \end{aligned}$$

The validity of the requirements for the Kalman filter of the yaw rate, vehicle speed and acceleration sensors can be read in [11].

The linear Kalman filter state estimation is computed in two steps: *prediction* and *correction*. Details can be found in [11], [14].



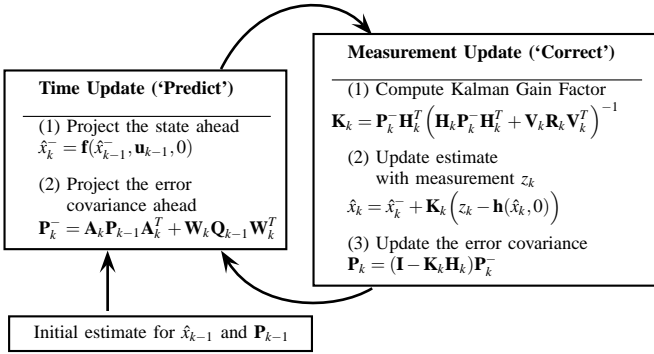
D. The Extended Kalman Filter

The extended Kalman filter is necessary if the state transition is non-linear, as in our case. Now the system is described by the non-linear, differentiable functions \mathbf{f} and \mathbf{h} :

$$\begin{aligned} \mathbf{x}(k+1) &= \mathbf{f}(\mathbf{x}(k), \mathbf{u}(k), \mathbf{w}(k)), \\ &= \mathbf{J}\mathbf{x}(k) + \mathbf{w}(k), \end{aligned} \quad (8)$$

$$\mathbf{z}(k+1) = \mathbf{h}(\mathbf{x}(k+1), \mathbf{v}(k+1)) \quad (9)$$

In our case, the measurement equation stays as in (7). The Extended Kalman filter state estimation is again computed in two steps: *prediction* and *correction*, but now with the linearized function.



E. GPS Data in UTM Coordinates

A standard GPS sensor was available for the recorded drives. The temporal resolution with 1Hz is not very high. Also the absolute position is not very accurate. There are often invalid sections from tunnels, synchronization problems, insufficient signal quality or too few satellites. Furthermore, there are severe outliers in the signal that are suppressed.

The UTM representation (cf. [10], [15]) of GPS has the advantage that the units use a metric world-coordinate system similar to the information obtained by the vehicle data. Map material from OpenStreetMaps was used for visualization.

F. Estimation of the Lateral Distance

As illustrated in Fig. 2, the yaw angle $\varphi(k)$ between the vehicle and the lane must be known in order to calculate

the lateral distance $l(k)$. The lane is estimated by the low-pass filtered vehicle trajectory using a 2nd-order Butterworth filter with cut-off frequency 0.05 Hz. The relative lateral displacement Δl related to the lane is calculated for every sampling period T . The lateral distance is then obtained by updating the estimated lateral position in each sampling period:

$$l(k+1) = l(k) + \Delta l \quad (10)$$

with the initial condition $l(0) = 0$. The lateral distance signal obtained from the vehicle model is again high-pass filtered to remove accumulating errors. Furthermore, it was low-pass filtered to remove noise and road influences with a 2nd-order Butterworth filter with the cut-off frequency 0.1 Hz.

III. FEATURE EXTRACTION

An overview about analyzed lane data based features and the methods how to extract them is described in [7]. This section will explain the features that were selected as potential features and for which the odometric data are sufficient.

A. Features

Tab. II lists the selected features investigated in the current study. Lane data based and odometric features are calculated with the same algorithms.

TABLE II
SELECTION OF LANE-BASED FEATURES

ID	Feature Name	Description
15	LANEDEV	Lane deviation
17	ZIGZAGS	Number of zig-zag events
29	LNMSQ	Lane mean squared
34	ORA	Overrun area
16	LATPOSZCR	Lateral position ZCR
30	LNIQR	IRQ of lateral position
37	DELTADUR	Duration between inflection points
38	DELTALATPOS	Mean lateral amplitude
39	DELTALATVELMAX	Max lateral velocity

B. System Active Signal

As the lane changes are not detected by the camera anymore, the turn indicator lever signal was used to suppress lane changes. Three seconds before and ten seconds after lever operation have been suppressed. Yaw rates $\dot{\psi} > 3^\circ/s$ have been neglected as well. Furthermore, the system was defined to be active only at velocities over 80 km/h.

IV. RESULTS

This section describes the comparison of the lane data and inertial-data based signals on a physical basis. The correlation of lane-based and odometric features is shown, as well as the correlation between the odometric features and KSS the drowsiness reference, using the Pearson and Spearman correlation coefficients.

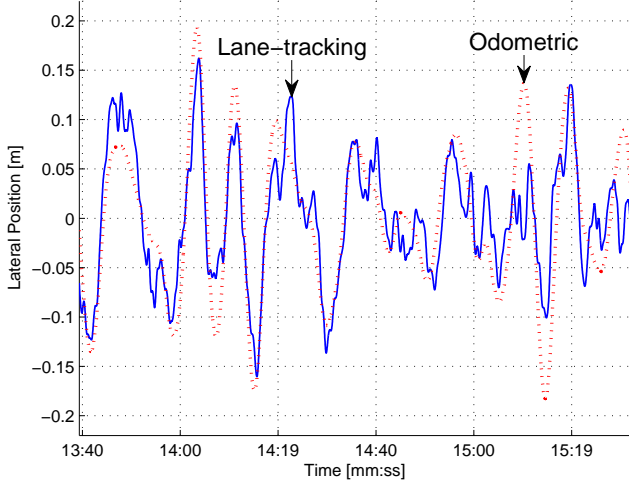


Fig. 3. Lateral position from lane-based (blue, solid) and odometric sensors (red, dotted)

A. Comparison of Lane Data and Inertial Data

Fig. 3 shows the lateral deviation (“distance”) signal obtained after removing the offset. However, the mean deviation between the two signals is 38cm which indicates that there are certain different influences in the signal.

The Spearman correlation coefficient between the yaw rate derived features and the original lane-based features are shown in Tab. III.

TABLE III
CORRELATION COEFFICIENTS BETWEEN LANE-DATA AND ODOMETRIC FEATURES

ID	Feature Name	ρ_p	ρ_s
15	LANEDEV	0.006	0.323
17	ZIGZAGS	1.000	0.515
29	LNMSQ	0.064	0.670
34	ORA	0.443	0.416
16	LATPOSZCR	1.000	0.770
30	LNQR	0.359	0.693
37	DELTADUR	0.573	0.389
38	DELTALATPOS	0.198	0.429
39	DELTALATVELMAX	0.593	0.536

B. Feature Evaluation

Features were assessed and optimized in multiple ways. Beside statistical tests, the *Bravais-Pearson correlation coefficient* ρ_p , *Spearman correlation coefficient* ρ_s and the *Fisher-metric MDA* [16] were used as metrics. ρ_p is calculated to estimate the linear correlation between the feature F_i and the interpolated, smoothed KSS

$$\rho_p(F_i, \text{KSS}) = \frac{\text{cov}(F_i, \text{KSS})}{\sqrt{\text{var}(F_i) \cdot \text{var}(\text{KSS})}}, \quad (11)$$

where *cov* is the *covariance* and *var* the *variance*. High positive/negative values mean strong positive/negative correlation, whereas a value near zero indicates a random relationship. The Spearman correlation coefficients work in

a similar way, just that non-linear correlation also results in high correlation coefficients. The Spearman correlation coefficient between the yaw rate derived features and the original lane-based features are shown in Tab. IV.

TABLE IV
SPEARMAN CORRELATION COEFFICIENTS BETWEEN LANE DATA AND INERTIAL DATA BASED FEATURES AGAINST THE KAROLINSKA-SLEEPINESS SCALE

Feature Name	ρ_s Lane vs. KSS	ρ_s Odom. vs. KSS
LANEDEV	0.211	0.046
ZIGZAGS	0.318	0.080
LNMSQ	0.177	0.080
ORA	0.325	0.105
LATPOSZCR	0.223	0.300
LNQR	0.187	0.100
DELTADUR	0.220	0.117
DELTALATPOS	0.239	0.079
DELTALATVELMAX	0.214	0.106

Fig. 4 shows the feature LANEDEV for a drive. The principal correlation between them can be roughly seen in this average example.

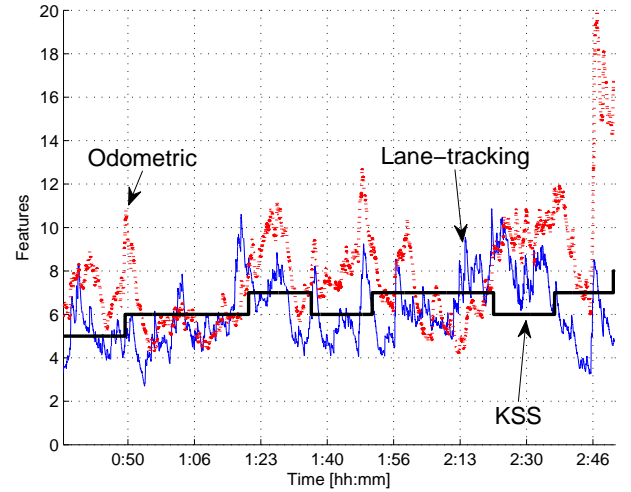


Fig. 4. Drive with the KSS sleepiness scale and the lane data (blue, solid) and inertial data (red, dotted) based feature LANEDEV.

Even if some features (ZIGZAGS and LATPOSZCR, zero-crossing rate) correlate very well with the lane-based pendant, they do not perform as good in regards to drowsiness detection. Just the feature LATPOSZCR performs better.

V. CONCLUSIONS AND FURTHER WORK

The basic motivation of the presented work is to estimate classical lane-based features solely from inertial sensors instead from camera-based lane data. In this paper, we present a comparison of these two methods. This has the benefit, that odometric data is nowadays found in almost every vehicle. In contrast, lane tracking cameras are special equipment and thus still rarely available in today’s fleet. Another major advantage of inertial data is its independence from weather,

camera calibration and lane-marking quality. This property highly increases the operability of the system. A motion model for inertial sensor signals using the extended Kalman filter was presented to derive the lateral lane deviation from odometric data. For a comparison and visualization of lane data and data derived from inertial sensors, GPS data was additionally used. As the GPS signal is only available every second whereas the CAN data has a cycle time of 20 ms, a method to include the GPS measurements into the motion model was proposed. Inertial and GPS data have been converted to the UTM coordinate system to have the same metric representation. This study shows that the features extracted from odometric data correlate well with the lane-based features. A large set of data was compared. However, there are relevant differences in the signal which make the exact estimation of the lane deviation impossible. The major problem remains the separation between road curvature and vehicle lurching between the lane markings. The nine "lane-based" features estimated by inertial data have been analyzed for their performance to detect impaired driving as explained in [7]. The correlation of the features with the Karolinska Sleepiness Scale drowsiness reference is comparable but inferior to the performance of real lane data based features. Generally speaking, some lane-based features can be approximated very well by odometric data whereas others cannot. Most odometric features do not perform as well as their lane-based equivalent. Only the LATPOSZCR (zero-crossing rate of lateral position) performs better, because of the continuous system availability of the inertial sensors.

A. Further Work

Current work investigates the mentioned problems by:

- Investigate if an approximation of further features (Time-to-Lane-Crossing and LANEAPPROX) is also possible with odometric data.
- Implement the approach in real-time to verify it.
- Improve the model and implementation details to improve the performance.
- Use the coupled tracking information for improved road condition analysis.

APPENDIX

A. Symbols

A	State transition matrix ($n \times n$)
B	Control input transition matrix ($n \times o$)
H	Measurement transition matrix ($m \times n$)
P	Covariance of the state vector estimate.
Q	Process noise covariance
R	Measurement noise covariance
$\mathbf{w}(k)$	Model/Process noise with covariance matrix W
$\mathbf{v}(k)$	Measurement noise with covariance matrix V
δ_{nk}	Dirac impulse $\begin{cases} 1 & \text{if } n = k \\ 0 & \text{otherwise} \end{cases}$

REFERENCES

- [1] E. Martin, "Breakthrough research on real-world driver behavior released," *National Highway Traffic Safety Administration*, 2006.
- [2] Daimler, "Hightech Report 2/2008 - Feature Attention Assist," 2008.
- [3] G. I. W. Duncker, "Jeder vierte Autofahrer sitzt übermüdet am Steuer," *Deutsche Ophthalmologische Gesellschaft e.V.*, Tech. Rep., 2007.
- [4] D. Künzel, *Die Rolle von Ablenkung und Müdigkeit bei Verkehrsunfällen: Nationale und internationale Statistiken*, Kuratorium für Verkehrssicherheit, 2008.
- [5] M.-L. Fertner, "Sekundenschlaf & Ablenkung," ÖAMTC - Der sterreichische Automobil-, Motorrad- und Touring Club, Tech. Rep., 2009.
- [6] T. Åkerstedt and M. Gillberg, "Subjective and objective sleepiness in the active individual," *International Journal of Neuroscience*, vol. 52, p. 2937, 1980.
- [7] F. Friedrichs and B. Yang, "Camera-based drowsiness reference for driver state classification under real driving conditions," *Proceedings of the IEEE Intelligent Vehicles Symposium*, 2010.
- [8] F. Friedrichs and B. Yang, "Drowsiness monitoring by steering and lane data based features under real driving conditions," *EUSIPCO*, 2010.
- [9] Clayton, "Klothoide," 2006. [Online]. Available: <http://ww3.cad.de/foren/ubb/uploads/Clayton/Klothoide-Formeln.pdf>
- [10] C. Hasberg and S. Hensel, "Online-estimation of road map elements using spline curves," *12th International Conference on Information Fusion*, 2009.
- [11] M. Bühren, "Simulation und Verarbeitung von Radarziellisten im Automobil," Ph.D. dissertation, Chair of System Theory and Signal Processing, 2008.
- [12] M. Miksch, B. Yang, and K. Zimmermann, "Motion compensation for obstacle detection based on homography and odometric data with virtual camera perspectives," *Proc. of the IEEE Conference on Intelligent Vehicles*, 2010.
- [13] E. Schmidt, "Drivers misjudgement of vigilance state during prolonged monotonous daytime driving," *Accident Analysis & Prevention*, vol. 41, pp. 1087–1093, 2009.
- [14] G. Welch and G. Bishop, "An introduction to the kalman filter," *University of North Carolina at Chapel Hill, Department of Computer Science*, 2006.
- [15] LVGB, "Abbildung und UTM - Koordinaten," *Landesamt für Vermessung und Geoinformation Bayern*, 2009.
- [16] M. Welling, "Fisher linear discriminant analysis," University of Toronto, Department of Computer Science, Tech. Rep., 2005.